An Economic Evaluation of Parasitic Losses and the Impact of Conformance Control on Parasitic Losses in an EGS Horizontal Well

Patrick Mays, William Fleckenstein, Hossein Kazemi, Kaveh Amini, Balnur Mindygaliyeva

GTO Technologies, Inc.

Colorado School of Mines

Keywords

Geothermal, Enhanced Geothermal Systems, EGS, Economics, Parasitic Losses

ABSTRACT

In this paper we present a mathematical model to evaluate the economic impact of parasitic losses on electrical generation opportunity costs due to frictional pressure losses and thermal losses in an EGS system. Specifically, we will evaluate the impact of rate vs. wellbore geometry (well length, casing size, number of hydraulic fracture stages, etc.) as well as doublet and triplet well systems. The analysis will quantify the economic costs of parasitic losses of the electricity generated by the facility and equipment that circulates water through the EGS. Additionally, we will evaluate the impact of conformance control measures used in oilfield waterfloods and why these techniques would not be economical in EGS.

We have presented a mathematical model to estimate the system parasitic power losses for a given flow rate. First, the frictional loss through a given pipe diameter is calculated with the Reynolds number. This method uses the Roughness of the pipe, and the pipe diameter to determine the friction pressure loss for different wellbore geometries at varying flow rates. The method then calculates the friction (or, equivalently the effective fracture permeability) in the induced fracture system. This model provides a deterministic basis of hydraulic horsepower requirements of the circulation system and the impacts of the circulating system's parasitic losses on an EGS development's economics. This evaluation includes the traditional conformance control methods of tubing, packers, and Injection Control Devices (often called Outflow Control Devices) on the energy requirements of the EGS circulation system.

This model demonstrates that the largest operating cost of an EGS system is the "Opportunity Cost" associated with using the generated carbon-free energy to run the circulating system. If this cost is not fully understood and modeled prior to deploying the EGS, the reduction of the salable

electricity could cause a significant impact to the economics. Furthermore, if traditional 'plug and perf' completion techniques do not provide the required conformance control and traditional methods of conformance control are required to manage injection, the frictional losses could be so great that the system requires more electricity than it generates.

In the paper first we examine the relative economic effects of the system circulation rates and wellbore geometric configuration on the opportunity costs of parasitic losses including the impact of post-facto conformance control, in addition to the typical operating cost estimate based on plant and field size. Second, we illustrate the need to properly model and understand parasitic losses prior to the design of the development plan for any EGS project. Third, we discuss the impact of alternative conformance control measures on the project economics.

1. Introduction

The heat within the Earth has been used to generate carbon free electricity since 1904 when the first geothermal power plant was built at the Lardorello dry steam field in Tuscany, Italy. From a humble beginning of 10 kilowatts (kW) of energy, Lardorello Geothermal Complex has grown to a capacity of 769 megawatts (MW) and currently it is the 2nd largest geothermal power plant in the world (Statista, 2024).

The current global geothermal power generation capacity is 16 gigawatts (GW), and the United States lead the world with 3.9 GW of geothermal power (Figure 1).

In the United States the Geysers Geothermal Complex is capable of producing 900 megawatts (MW) of electricity through its 18 power plants. However, even with the tremendous resources like the Salton Sea and the Geysers Fields in California, the Mean Net Generation of geothermal electricity in the United States has stagnated between 1.5 GW and 1.9 GW since 1990 (Robins, et al. 2021).

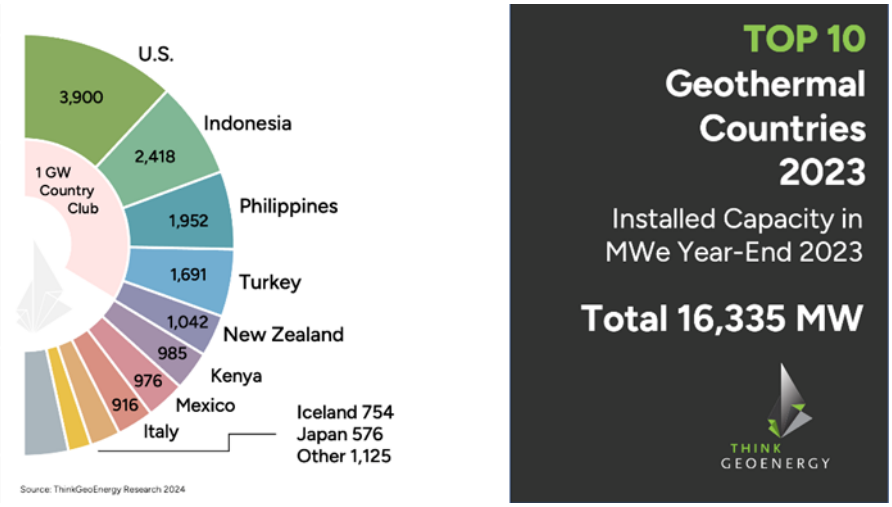

Figure 1: Top 10 geothermal countries in the world as of 2023 (ThinkGeoEnergy, January 2024).

The primary cause of this stagnation in growth is because the main source of the geothermal power in the world is from subsurface hot water reservoirs known as hydrothermal resources where the reservoirs' high temperatures and permeabilities provide natural or pumped flow of superheated

water to the surface for economical generation of electricity. Unfortunately, scarcity of hydrothermal fields and the trifling discovery of new fields that can significantly grow carbon-free power to offset current declining fields are the reasons for non-growth of hydrothermal reservoirs. It is estimated that only 2% of the geothermal resources in the world are accessible using hydrothermal technology (Geiser, Marsh and Hilpert, 2016). Between 2016 and 2021, eleven (11) plants were taken offline, removing 103.3 MW of nameplate capacity and only seven (7) new plants have gone online during this time supplying 186.3 MW of nameplate capacity (Robins, et al. 2021).

In an attempt to grow geothermal power generation beyond the limits of hydrothermal systems, there has been a great deal of research and development resulting in advances in a newer form of geothermal power generation referred to as Enhanced (or Engineered) Geothermal Systems (EGS). In contrast to the high-permeability hydrothermal systems, the EGS heat reservoirs typically consists of hot-dry-rocks with extremely low porosity, permeability; and no water is present in the limited pore spaces. This resource is referred to as Hot Dry Rock (HDR). To produce heat from an HDR, a subsurface heat exchanger must be created. Water can be injected into this subsurface heat exchanger and circulated to extract heat from the rock. Specifically, one creates an artificial link between 2 or more horizontal bore holes using hydraulic stimulation technology to allow cold water to be pumped down an "injector" well to a depth of sufficient geothermal heat. Once at depth, the water will be heated within the fracture network by the surrounding rocks to a temperature sufficient to generate electricity. The heated water will then be recovered to surface via the producer(s) and typically run through an Organic Rankin Cycle (ORC) plant to generate carbon free electricity

The key enablers to EGS are step change technology advances in extended reach, horizontal drilling and multi-stage hydraulic fracturing due to the development of shale hydrocarbon resources. Wells that with a true vertical depth (TVD) of 9,000 ft and a lateral departure of greater than 5,000 ft horizontally are now being drilled in under 25 days, in rocks that 7 years ago would have taken over 90 days to drill at 3 to 4 times the cost. In addition to drilling and stimulating the wells, the EGS systems require continuous injection of water into the target hot rock zone because of the absence of water in such systems (Mindygaliyeva, et al. 2024).

The availability of a water source for use in the EGS presents multiple challenges that must be examined for any EGS development project to be economically successful. First, access to the source and quantity of water for well stimulation (i.e., hydraulic fracturing) and fluid circulation must be established as part of project selection. Second, daily rates and volumes circulated to generate electricity to be economically viable must be understood. Third, modeling the required horsepower to run the circulation system and the potential impacts on for-sale-electricity (referred to as parasitic losses). Fourth, managing conformance control solutions (to distribute water evenly in the hydraulic fracture flow paths) and their impact on parasitic losses and thermal decline.

2. Key Variables Impacting Economics in an EGS System

Several key variables impact the economics of EGS. These variables were evaluated stochastically (Fleckenstein et al, 2023). The three dominant independent variables in EGS economics are (1) thermal decline, (2) flow rate per well, and (3) Power Purchase Agreement (PPA) pricing. It is not the intent of the current analysis to project what PPA pricing to use in economics, nor to project how long the current tax credits will last, nor whether carbon credits will enter the United States

market the same way as in the European Union. Rather, using a fixed set of assumptions for these variables, this analysis focuses on the thermal decline and flowrate per well to understand their impact on the net power production.

2.1. EGS System Heat Extraction Fundamentals

For an EGS system to successfully function, a minimum of two horizontal wellbores must be interconnected through a system of fracture stimulations. When there is one injector and one producer in a pair, the system is referred to as a "doublet" (Figure 2). It is critical that controlled water flow passed from the injection well to the production well as evenly as possible across the fracture system. As the water flows through the fracture to the production well, the geothermal energy from the Earth heats the fluid. The hot water flows up the production well and is converted into electricity at the surface using an ORC.

The alternate EGS system to the doublet is the 'triplet'. The concept of the triplet is that there is a single injector flanked on each side by a producer, creating a one injector, two producer system (Figure 3). The fractures are generated from the injector and will grow out radially in the direction of the maximum horizontal stress. If the two producers are correctly orientated on either side of the injector, perpendicular to the principal maximum stress, the fracture "wings" will intercept both producers. A properly engineered triplet system is ideal from a cost perspective, because only 1 set of stimulations from the injector can connect it to two producers, thus reducing completion costs by 50% and reducing the need to drill a second injection well.

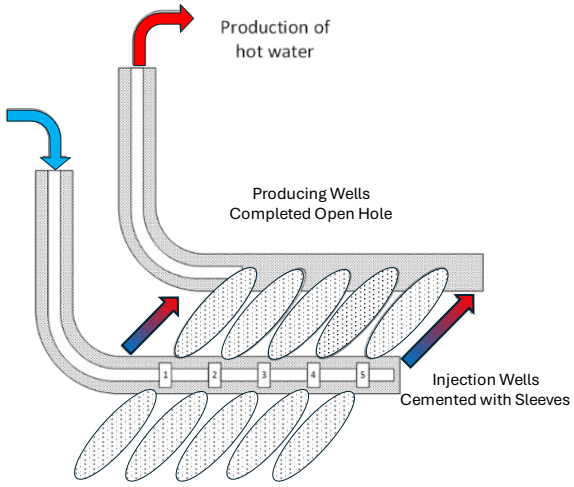

Figure 2: Doublet EGS Well System

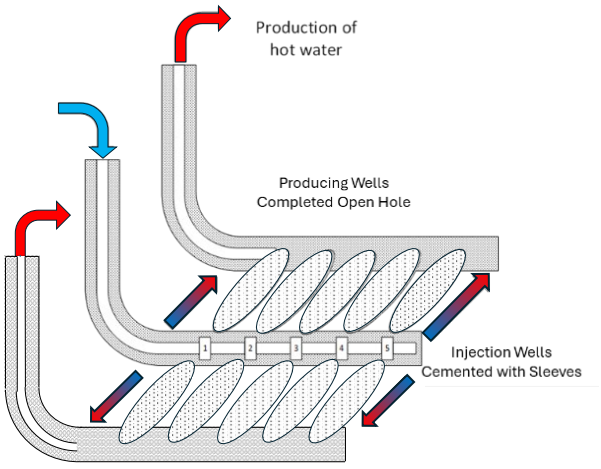

Figure 1: Triplet EGS Well System

2.2. Estimating Power Conversion and Required Flow Rate

The analysis method used starts by understanding the initial resource temperature (T_{r0}, in this analysis assumed to be the same as the plant input temperature for simplification) by drilling a regional exploration well. Once the temperature profile is understood, the required flow rate per well is calculated to design the subsurface system rate to match the power generation, in this case

the ORC. Starting with a base assumption that systems of 5 MW per doublet or 10 MW per triplet are required to be economic. Two methods were used to determine the estimated flow rate based on the resource temperature.

A common source to predict power from a binary plant (e.g., an ORC system) is to use equation 7.1 by Tester published in the 2006 MIT-led report (MIT led interdisciplinary panel 2006) where Tester extrapolated the thermal efficiency (η_{th}) based on the geofluid temperature of eight operating binary plants. Tester's linear regression resulted in the following formula for thermal efficiency (MIT led interdisciplinary panel, 2006):

$$\eta_{th} = 0.0935\,T - 2.3266 \quad (1)$$

Where,

$\eta_{th} = thermal\ efficiency,\ \%$ (For reservoir temp 90 ^{o}C - 250 ^{o}C $\Rightarrow$ 6 *to* 21%)

$T = Temperature\ of\ produced\ fluid,\ ^{o}C$

The equation for calculating electric power:

$$Q = \dot{m} c_w \Delta T \quad (2)$$

Where,

Q = electric power (J/s)

$\dot{m}$ = mass flow rate entering power generation turbine (kg/s)

c_w = specific heat of water (J/(kg·˚C)),

$$\Delta T = inlet\ T - Outlet\ T, (^{\circ}C) \quad (3)$$

Considering thermal efficiency of power plants, we can calculate the megawatt output of the plant using the following equation:

$$Q\eta_{th}/1{,}000{,}000 = plant\ power, MW \quad (4)$$

Utilizing the average plant ΔT of 73˚C (Moon et al, 2012) in plants greater than 150˚C and less than 250˚C, the required production rate to generate 5 MW can be solved for the assumed initial reservoir temperature T_{r0} of 205˚C at 60,200 BWPD per producer. Note, that the injection rate must account for formation fluid loss as documented at Blue Mountain (Norbeck and Latimer 2023). In this analysis it is assumed a fluid loss to formation of 8%.

As a validation check against Tester's formulas, the power conversions factors from Moon (Moon and Zarrouk, 2012) were evaluated for the same data set of plants greater than 150˚C and less than 250˚C. This resulted in an average power conversion factor of 4.72E-07 MW-hr / (˚C·BWPD) and a resulting rate per producer of 51,700 BWPD for 5 MW, representing a 16% difference from Tester's equation. For the Gringarten model used in this paper, the average of the two rate predictions of 56,000 BPD was used with a power conversion factor of 4.36E-07 MW-hr / (˚C·BWPD).

It is important to note that ~200˚C is recognized as a critical break over point between flash systems and binary systems. If a flash system is used, the efficiency of the plant could potentially reach 31% as documented by an MIT led interdisciplinary panel (MIT, 2006). However, this efficiency will have to be derated assuming that the cooling tower is replaced with air cooling to maintain 100% capture of the fluids for reinjection. Flashing also brings additional scaling issues for the plant depending on the water chemistry and must be evaluated on a case-by-case basis. For these reasons, all assumptions in this analysis use ORC power plants.

2.3. Modeling of a Subsurface Heat Exchanger

Modeling of subsurface heat exchanger is the same for both the 'doublet' and 'triplet'. In a typical EGS system, the wells are drilled to a formation that has a geothermal temperature of 200˚C to 260˚C. As the fluid is injected into the well it will slowly increase in temperature with depth. Once the fluid exits the wellbore the fluid is forced through the fracture where the heat from the earth will raise the temperature of the fluid to approximately the same temperature as the formation. The water will continue to the production well where it is produced back to surface for conversion to electricity. The temperature of the water will slowly decrease as it travels to the plant as a function of depth, wellbore geometry, flowrate, and ambient temperature. This can be countered through various insulation technologies in the market, such as vacuum insulated tubulars and cement with low thermal conductivity. For simplicity in this model, the bottom hole outflow temperature has been assumed as the same as the surface temperature.

The basis of modeling the heat exchanger using horizontal wells with multiple fractures in a reservoir was first developed by Gringarten, (Gringarten et al., 1975), and further advanced by Doe (Doe, McLaren and Dershowitz, 2014). Gringarten's heat extraction model was based on a set of parallel fractures with uniform properties—including fracture height (y), length (z), transmissibility (T), flow rate (q), and fracture half-spacing (xe). The length (z) represented the distance from the injector to the producer, and the total length (x) represented the horizontal length of the wellbore with the model allowing for a variable number of fractures (n) (Figure 4).

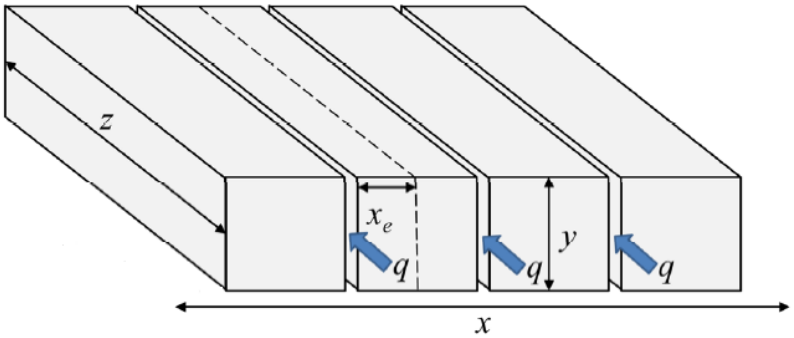

Figure 4: Gringarten et al. model, modified by Doe et al. (Augustine, 2016).

Using this model Gringarten developed a solution for thermal modeling an EGS system using dimensionless produced temperature (T_{wD}), dimensionless time (t_D), and dimensionless half-fracture spacing (X_{ED}), later simplified by Doe (Doe, McLaren and Dershowitz, 2014).

$$T_{wD} = \frac{T_{Ro} - T_w(z,t)}{T_{Ro} - T_{wo}} \tag{5}$$

Where

$T_w(z,t)$ = water temperature at z and t, ^oC
T_{Ro} = intilal rock temperature at point of injection, e.g., 300^oC
T_{wo} = water injection temperature, e.g., 40^oC

$$t_D = \frac{(\rho_w c_w)^2}{K_R \rho_R c_R}\left(\frac{q}{z}\right)^2 (t - \frac{z}{v}) \cong \frac{(\rho_w c_w)^2}{K_R \rho_R c_R}\left(\frac{q}{z}\right)^2 t \quad (6)$$

Where,

q = volumetric flow rate per fracture per unit thickness in y direction, cm^3 / s
($e.g.$,1.45 x $10^5 cm^3 / s$)
z = distance above the injection point, cm
v = water velocity in fracture, cm/s
t = time, s
ρ_w = *water* density, g/cm^3; e.g., 1.0 g/cm^3
c_w = *water specific heat*, $cal/(g.^oC)$; e,g., 1.0 cal/(g.^{o}C)
ρ_R = *rock* density, g/cm^3; e.g., 2.65 g/cm^3
c_R = *rock specific heat*, $cal/(g.^oC)$; e,g., 0.25 cal/(g.^{o}C)
K_R = *rock* thermal coductivity, cal/(cm.s.^{o}C) ; e.g., 6.2 x 10^{-3}cal/(cm.s.^{o}C)

$$x_{ED} = \frac{\rho_w c_w}{K_R}\left(\frac{q}{z}\right) x_E \quad (7)$$

Where,

x_E = *fracture spacing*, *cm*; *e.g.*, 4,000 *cm*

Using these dimensionless values and assumed uniform properties, Gringarten published these type curves for solving thermal decline based on reservoir properties and flow rates (Figure 5).

As noted by Doe, the function of thermal decline depends on the mass flow rate in the fracture vs. thermal diffusion rate from the rock matrix to the fractures (Figure 6). If the flow rate is too high within the fracture, it will travel faster than the rock matrix can supply heat to the fracture face. Alternatively, at lower flow rates, the thermal front in the matrix is better able to keep up with the rate of fluid flow in the fracture, causing a slower decline response, but steeper decline once it starts.

There must be a balance as fluid is pumped past the down hole heat exchanger to maintain the low-rate thermal front of Figure 6. Premature thermal decline from the high-rate thermal front can be caused by two events. The first event is pumping too much water down the injector compared to

the relative amount of fracture face surface area the system has, causing the entire system to prematurely decline. The second is a lack of conformance control, where the correctly calculated amount of water is pumped downhole, but it is preferentially traveling down a small subset of fractures, causing these fractures to prematurely cool, impacting the average outlet temperature's decline. This event is often referred to as '***short circuiting***'.

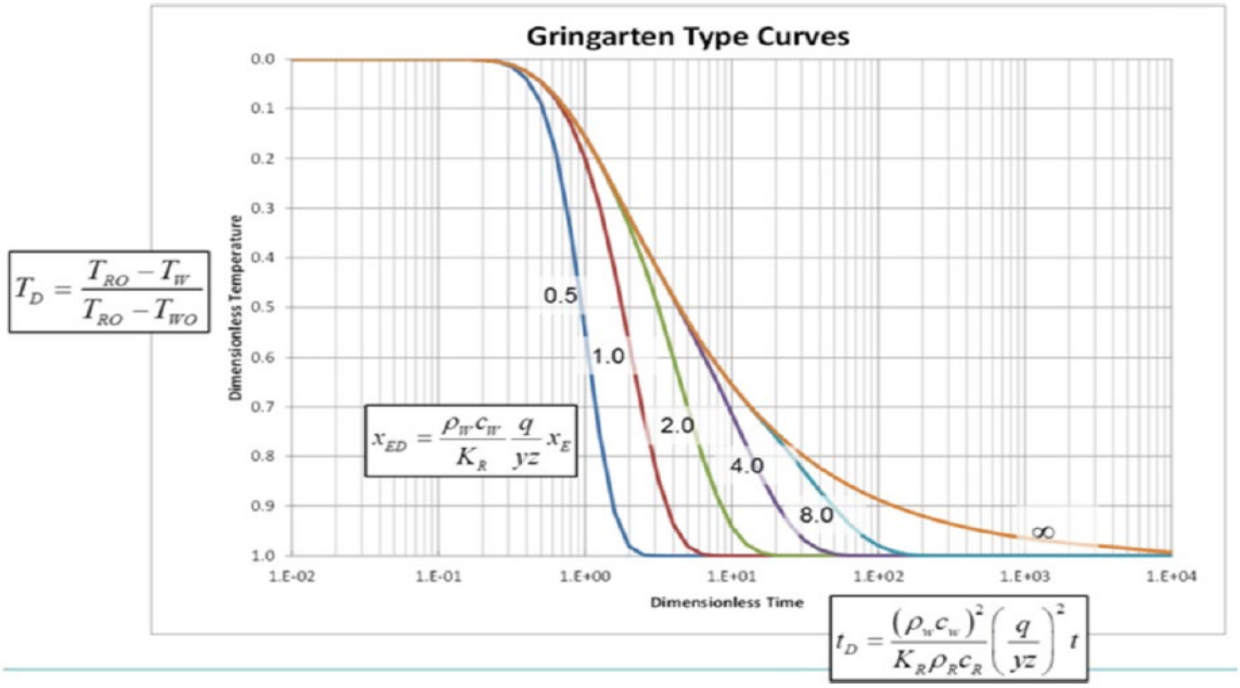

Figure 5: Gringarten type curves (Augustine, 2016).

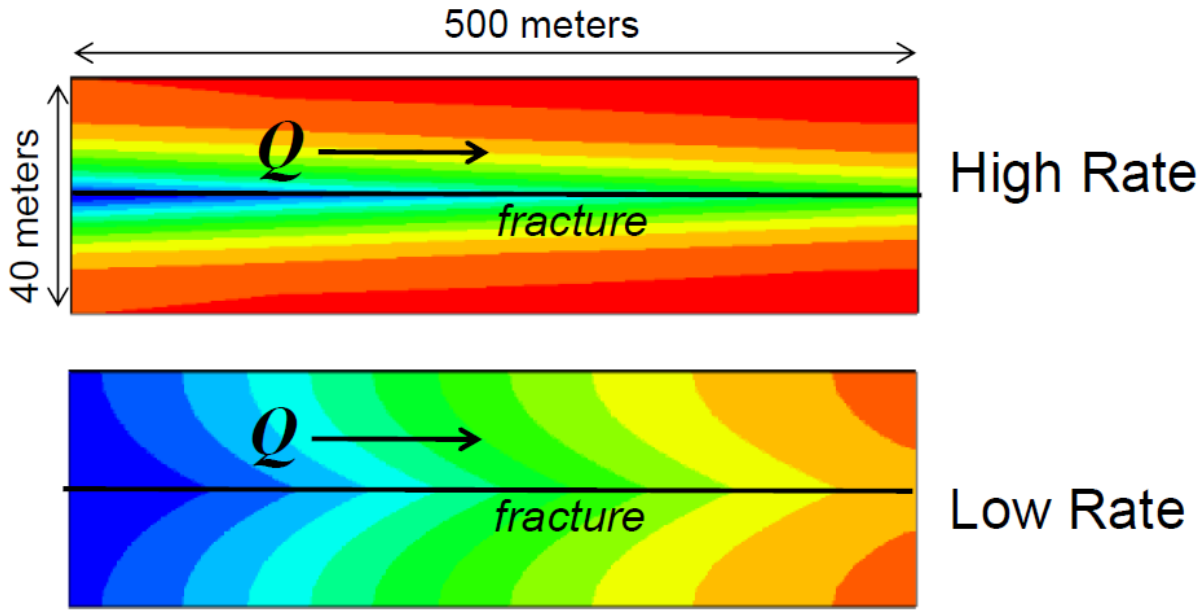

Figure 6: Diagram of thermal front vs flow rate (Doe, McLaren and Dershowitz, 2014).

Using the work established by Gringarten et al., and Doe et al. for a simplified model, a theoretical EGS was designed to model the thermal decline of a system. Using the parameters in Table 1, a "doublet" EGS system was modeled.

Table 1: EGS Parameters for Gringarten Thermal Decline

Density of Water	ρ_w	874 kg/m^3	
Heat Capacity Water	c_w	4180 J/Kg˚C	
Thermal Cond. Rock	K_R	3.00 J/m˙s˙˚K	
Density of Rock	ρ_R	2750 kg/m^3	
Heat Capacity Rock	c_R	790 J/Kg˚C	
	C_1	2.05E+06 s/m^2	
	C_2	1.22E+06 s/m^2	
number of fractures	n	55	
frac 1/2 spacing	Xe	21.9 m	72 ft
Frac spacing	2Xe	43.9 m	144 ft

Horizontal length	X	2414 m	7920 ft
spacing between horizs.	y	220 m	722 ft
Frac height (penny fracs)	Z	440 m	1444 ft
Total Flow Rate	q	0.103 m^3/s	56,000 BPD
Initial Reservoir Temp	T_{R0}	205 ˚C	478 ˚K
Abandonment Temp	T_w	164 ˚C	437 ˚K
Reinjection Temp	T_{w0}	60 ˚C	333 ˚K
Dimensionless Outlet Tem	T_{wD}	0.28	
Dimensionless 1/2 space	X_{eD}	0.52	
Dimensionless time	t_D	0.73	
Desired life	t	30 years	9.46E+08 seconds

Using the dimensionless variables, a graph of temperatures vs time was created (Figure 7); then, regression analysis was conducted to obtain Eq. 7. This equation and others were the basis for the economic model and subsequent calculations.

$$T(t) = -0.0009t^3 - 0.0279t^2 + 0.4193t + 204.06 \quad (t \text{ in years}) \tag{8}$$

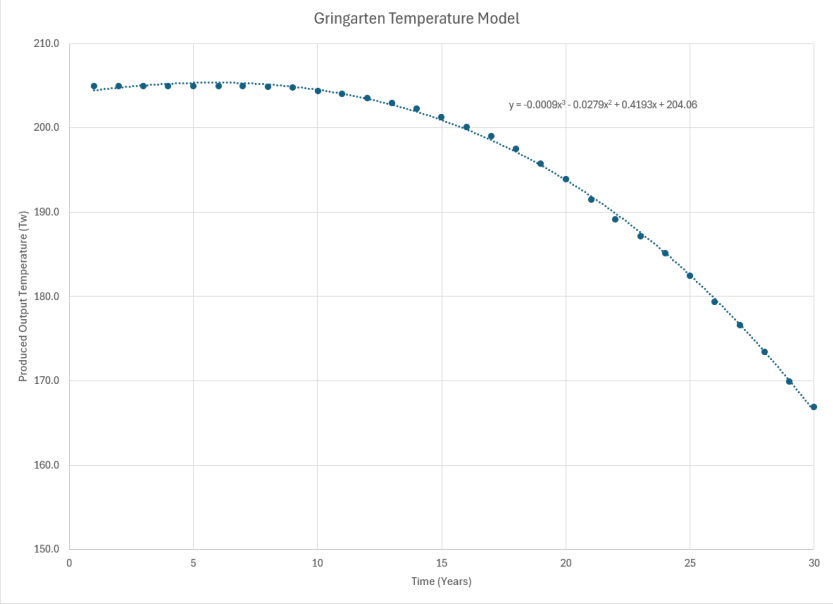

Figure 7: Thermal decline of theoretical EGS using Gringarten's model (Gringarten et. al., 1975).

There is criticality of designing an ORC to optimize the pinch point between the produced water and the working fluid. Understanding that the plant can be optimized for initial production based on the data gained in the exploration well, as the thermal decline occurs the plant efficiency will decrease, this is graphically depicted in figure 7.7 of the MIT report for flash plants. The economic model's maximum Temperature decline is 40˚C, as compared to Augustine's maximum decline (Augustine, 2011) of 32˚C. However, to account for the thermal decline and for the separation from the pinch point, the economic model assumes a linear 1.2 % loss in power generation for

every 1˚C drop in thermal decline, severely decreasing the electrical output in later years. In actual operations, similar to oil and gas fields, "infill" wells will most likely be drilled starting in year 20, to deeper, untapped resources to maintain higher heat, extending the plant life to 40+ years for a marginal cost.

2.4. Defining and Quantifying Parasitic Losses

Within the hydrothermal industry, parasitic loads are the electrical loads required to run the binary pumps, cooling tower fans, lighting, control room, and other equipment on site necessary to run the facility (DiPippo, 2016), typically around 8%. However, many economic models assume a fixed operating expense and overlook the variability of power needed (and associated costs) that EGS systems require due to the power required for the circulation of a significant amount of water. In the Gringarten model above, the required water circulation is estimated to be over 11,000 barrels of water per day (BWPD) for every MW of electricity produced at 205˚C. Previously, water circulation loads were calculated to be as high as 10% (Banks, et al., 2020) in Clarks Lake. However, this analysis was not for deep horizontal wells and considered friction loss to be insignificant. In deep, horizontal EGS systems, friction must be considered.

In this analysis, it is assumed that the resource is 9,845 ft deep, requires a horizonal lateral length of 7,920 ft, 55 frac stages, at a spacing of 144 ft between stages, with a total flow rate of 56,000 BWPD (~1,020 BWPD per frac). Later, these dimensions will be used with various wellbore architectures to demonstrate the frictional impact and resulting parasitic losses on EGS through Nodal Analysis.

Calculating the friction of the system for the parasitic losses was developed through a process of nodal analysis, using the inside diameter and the roughness of the tubulars combined with the density and viscosity of water (at temperature) and the friction within the fractures themselves. These properties were used to calculate the Reynolds numbers and Moody Friction Factors to generate the head loss in each node which was converted to psi. Six models were created for 9-5/8" 47ppf casing; 7" 35ppf casing; & 4" 11ppf tubing, each at 60˚C for injection and 205˚C for Production. These curves are identified in the appendices.

Once the friction loss models were created, the program was able to generate wellbore profiles with the following dimensions for both the producers and injectors (unless noted):

7" casing across the reservoir with 9-5/8" casing to surface

7" long string from TD to Surface

4" 'conformance string' across the reservoir with 9-5/8" casing to surface

4" 'conformance string' across the reservoir with 7" casing to surface

It is important to note that for casing burst calculations during stimulation, we required a burst strength of greater than 10,000 psi across the reservoir. Combining this requirement with the impact of thermal cycling on high strength alloys we did not evaluate 9-5/8" across the reservoir. This may be possible with special alloy tubulars.

The nodal model then calculated the frictional impact across the tubulars to the top of the reservoir, then the friction to each fracture initiation point based on the distance between stages. As the flow in the wellbore decreased at each node, the model calculated the new friction loss to the next fracture initiation point until the end of the well was reached.

To calculate the friction loss through the fractures the results from Blue Mountain were evaluated using the relationship of pressure drop/ft of fracture (modified to fracture ½ length since the project was a doublet) vs BPD fluid/ft fracture height, (Pearson, 2001). According to Titov (Titov, et al. 2023) the average fracture height was estimated at 800 ft and the average fracture half-length was estimates at 800 ft using micro seismic and fiber optic data. However, the average distance between wells was estimated at 365 ft and the effective fracture height was estimated to be 300 ft by Norbeck (Norbeck and Latimer 2023) and these numbers were used for the calculation. Using this data from Norbeck, to get the injection pressure vs rate and corresponding production rates and pressures, the model described above used nodal analysis to solve for the pressure losses in the fractures to generate Figure 8. The resulting model and regression for friction loss was history matched against Blue Mountain and found to be accurate.

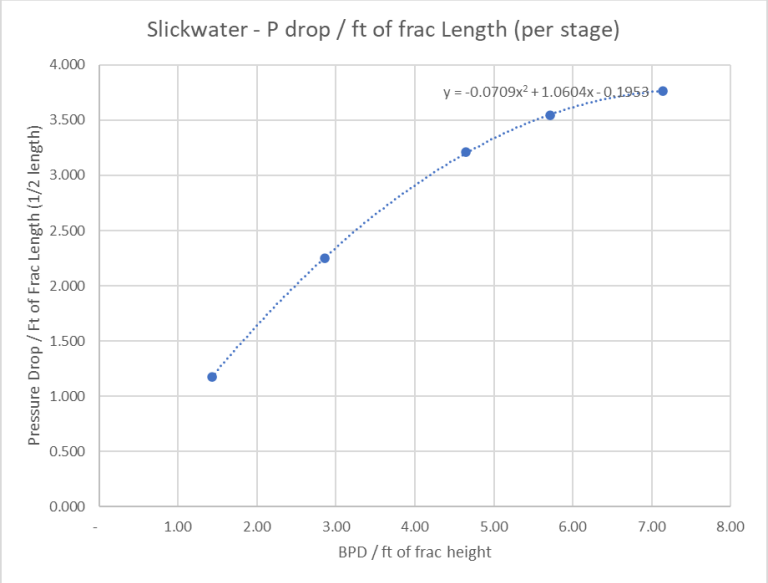

Figure 8: Calculated friction losses in the fractures of Project Red using 70/140 equivalent proppant.

Using API data, (Pearson, 2001), it is well established that the permeability of ceramic proppant, or even 30/50 Ottawa sand is significantly higher than the 70/140 equivalent sand that was pumped at Blue Mountain. At a closure stress of 5,000 psi, the API permeability of 40/70 bauxite is over 7 times greater, and 30/50 Ottawa is 2.4 times greater. One then can make a modest assumption that with improved fracturing technology the pressure losses within the fracture could be reduced by 66%. Thus, in our example with 56,000 BWPD traveling through 55 fractures, this change in proppant could have a required pressure decrease for the system of over 300 psi.

Using the same methodology outlined above for the friction losses returning up the producer, the entire pressure loss of the system can be calculated and the required HHP calculated for either a doublet or a triplet and used to define the system's parasitic losses.

Using the hypothetical doublet used in Gringarten's thermal model, and the well architecture described in Norbeck's paper (Norbeck and Latimer, 2023) on Blue Mountain, the pressure drop with a 7" long string from Surface to TD in both the injector and the producer can be calculated. Using a reservoir depth of 9,845 ft (3,000 m) and a lateral length of 7,920 ft, with 55 fractures, 144 ft between fractures and 56,000 BWPD the model can calculate the expected pressure drop in the system. In this scenario the expected pressure drop of the system is 3,104 psi.

$$HHP = \frac{P_{pump}(psi) \cdot q_{inj}(gpm)}{1714} \tag{9}$$

For example, an injection rate of 1,764 gpm and pressure drop of 3,104 psi, the required HHP to run the circulating system is 3,130 HP.

2.5. Thermal Decline

The concept of accelerated thermal decline due to "Short Circuiting" was further examined by Doe (Doe, McLaren and Dershowitz 2014). The team analyzed thermal decline using the initial Gringarten model (Gringarten, Witherspoon and Ohnishi, 1975) with 10 uniform fractures, then refined the model further by adding variations:

(a) Initial model (for direct comparison to Gringarten) :10 uniformly spaced, parallel fractures with uniform apertures.

(b) As (a), with variable fracture spacing and constant fracture transmissivity (aperture assumed based on a cubic law).

(c) As (b), Variable fracture spacing and lognormally distributed fracture transmissivity.

(d) As (c), with increased aperture coefficient of variation.

(e) As (c), with decreased aperture coefficient of variation.

(f) As (c), with fractures defined by a distribution of fracture size, orientation, and intensity based on a field case study.

The first analysis looked at 10 uniform fractures with varying fracture spacing to understand the impact on spacing assuming a total flow rate of 0.15 m3/s (81,500 bbl/day), or a rate per fracture of 0.015 m3/s (8,150 bbl/day) for 1,000 m x 1,000 m fractures (Figure 9).

Doe noted two major effects by modeling the scenarios (b) through (f) above. First, the temperature maps show that thermal interference and more rapid thermal depletion occurs in areas of great fracture density. This is independent of the aperture or fracture conductivity. The second observation was that variable apertures create variable breakthrough times or 'short circuiting' among fractures with considerably more aperture or fracture conductivity, Figure 10.

Doe found that using a variable aperture negates much of the advantage of distributing flow over multiple fractures that the Gringarten model predicts due to the second power relationship of dimensionless time to rate. This data was plotted on the familiar outlet temperature vs. time and the impact of the thermal decline from 'short circuiting' could be visualized, Figure 11.

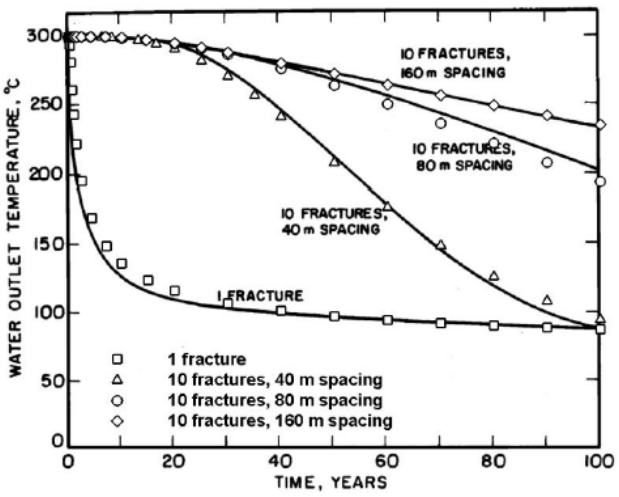

Figure 9: Water outlet temperature for Gringarten example with Frac Spacing increasing (Doe, McLaren and Dershowitz 2014).

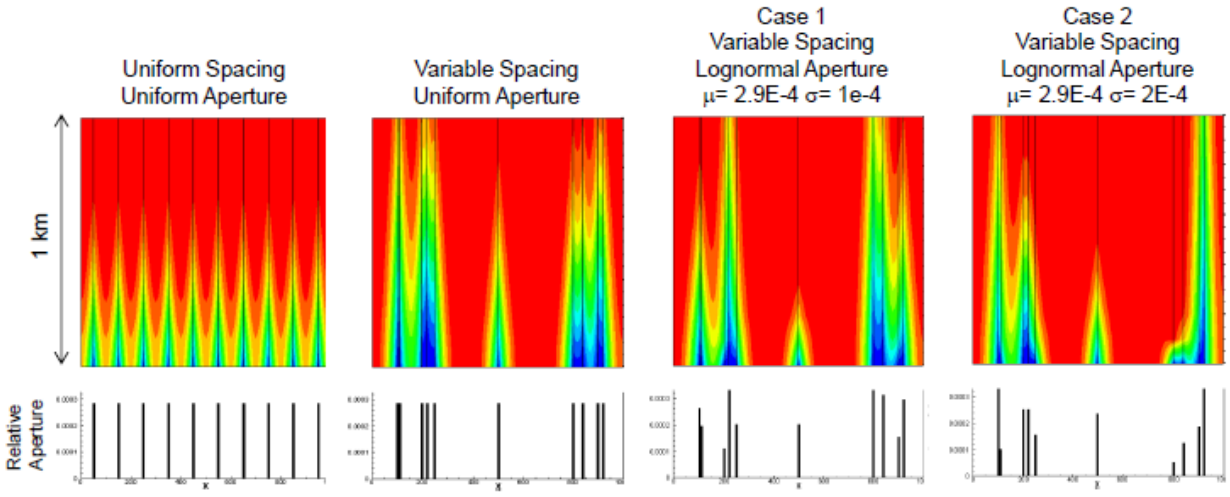

Figure 10: Heat maps for parallel fractures using variable spacing and fracture conductivity (Doe, McLaren and Dershowitz, 2014).

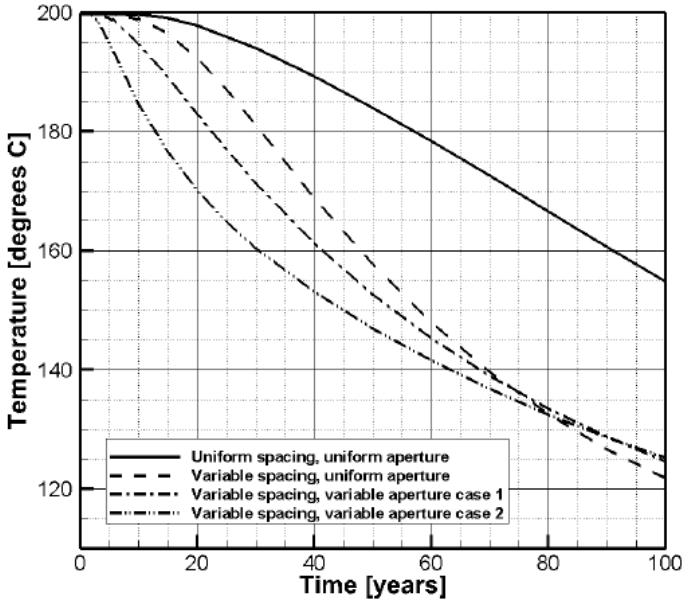

Figure 11: Impact on temperature output for variable fracture spacing and fracture conductivity (Doe, McLaren and Dershowitz, 2014).

2.6. Predicting Thermal Decline

The EGS project at Blue Mountain has fundamentally changed the EGS industry. For the first time, models created by early innovators can be compared against actual data from an EGS site that uses a horizontal injector and producer connected by multiple fracture stimulations. The two wells were drilled to a vertical depth of approximately 7,700 ft., and each had a horizontal lateral section of roughly 3,250 ft. Both wells had 7", 35 ppf, P-110 production casing run from surface to TD. The average offset spacing was 365 ft. The Injector was completed with a total of 16 stages with each stage having approximately 150 ft. All stages except stages 12 and 13 had 6 clusters per stage and 6 shots per cluster. Stages 12 & 13 had 9 clusters per stage and variable shots per cluster. The proppant was a mixture of 100 mesh and 40/70 mesh silica sand. The producer was completed in a similar technique with a total of 20 stages.

The first published injection profile from Blue Mountain showed just how different the reality of the injection profile is as compared to Gringarten's very simplified model of uniform fractures. Of approximately 18,100 BWPD of injection during the spinner survey there was a wide discrepancy of water per stage. Table 2 and Figure 12 show the stage, vs water injection allocation at Blue Mountain EGS.

Table 2: Blue Mountain Injection allocation

Stage	Approximate Injection Allocation (BWPD)
1	1,150
2	250
3	1,000
4	100
5	1,300
6	1,650
7	600
8	2,000
9	2,100
10	2,550
11	400
12	1,000
13	1,200
14	1,100
15	700
16	1,000
Total	18,100

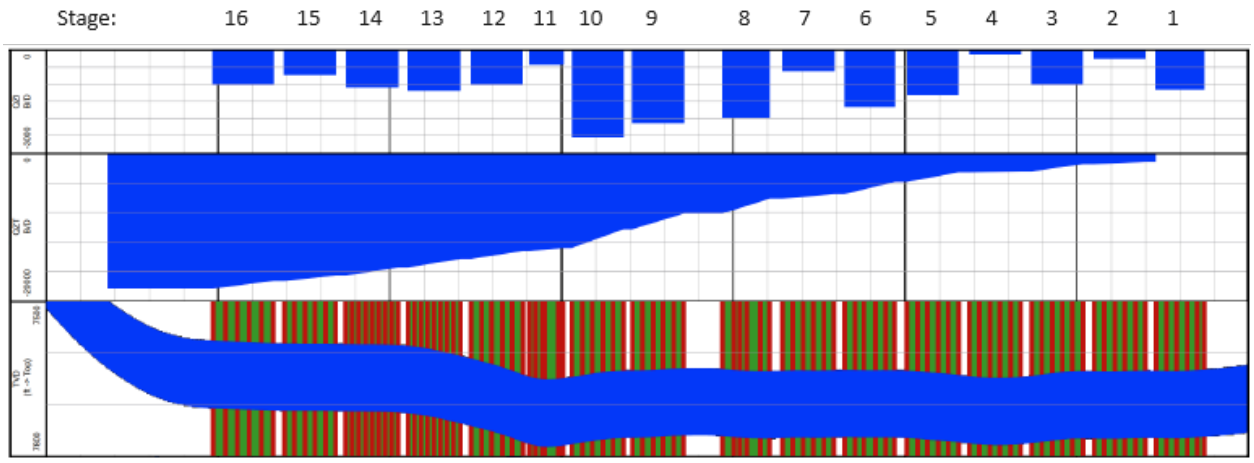

Figure 12: Blue Mountain spinner survey showing the amount of fluid allocated to each frac cluster (Norbeck and Latimer 2023).

2.7. Economic Impact from a Lack of Conformance Control

Using the data generated at the Blue Mountain site combined with the Gringarten Model, the predictions generated by Doe et al. can be evaluated and put into an economic model. The flow rates noted above were distributed into quartiles for the evaluation (Figure 13).

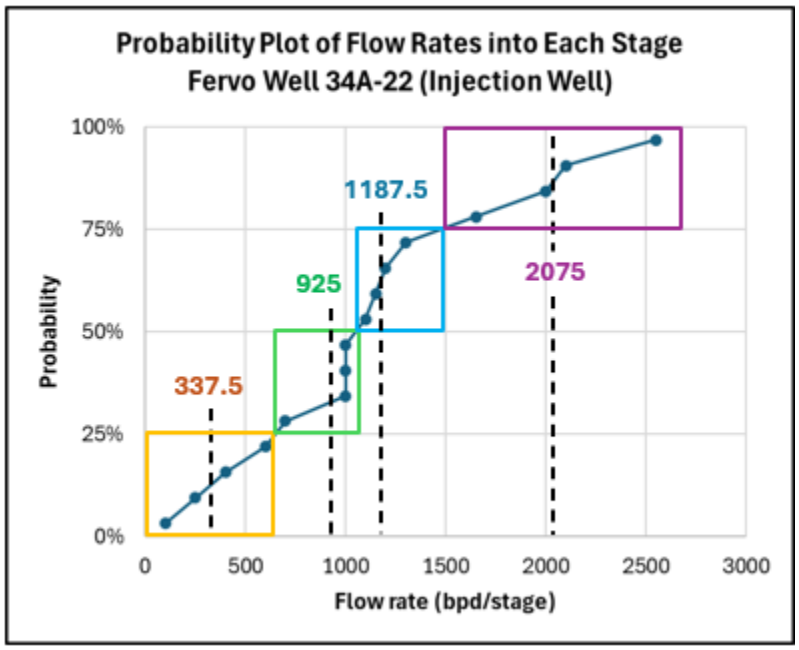

Figure 13: Flow distribution at Blue Mountain by quartiles.

Using the resulting flow rates per stage for each quartile, the flow distribution can be allocated to our theoretical well's Gringarten model using the following Table 3.

Table 3: Allocation of flow for Gringarten Model based on Blue Mountain

Flow Stream	FERVO Blue Mountain Project		This Paper
	Flow Rate (bpd/stage)	Normalized Rate (Rate/Avg. Rate)	Flow Rate (bpd/stage)
1st Quartile	338	0.298	304
2nd Quartile	925	0.818	832
3rd Quartile	1,188	1.050	1,068
4th Quartile	2,075	1.834	1,867
Average	1,131	1.000	1,018

These flow rates were then proportionally distributed into the theoretical well using Gringarten type curves. Using MATLAB, thermal decline curves were generated for each set of fracture by interpolating dimensionless time, dimensionless temperature and dimensionless half-fracture spacing. The decline for each quartile and the composite thermal decline using flow balance was plotted against the original Gringarten curve in Figure 14.

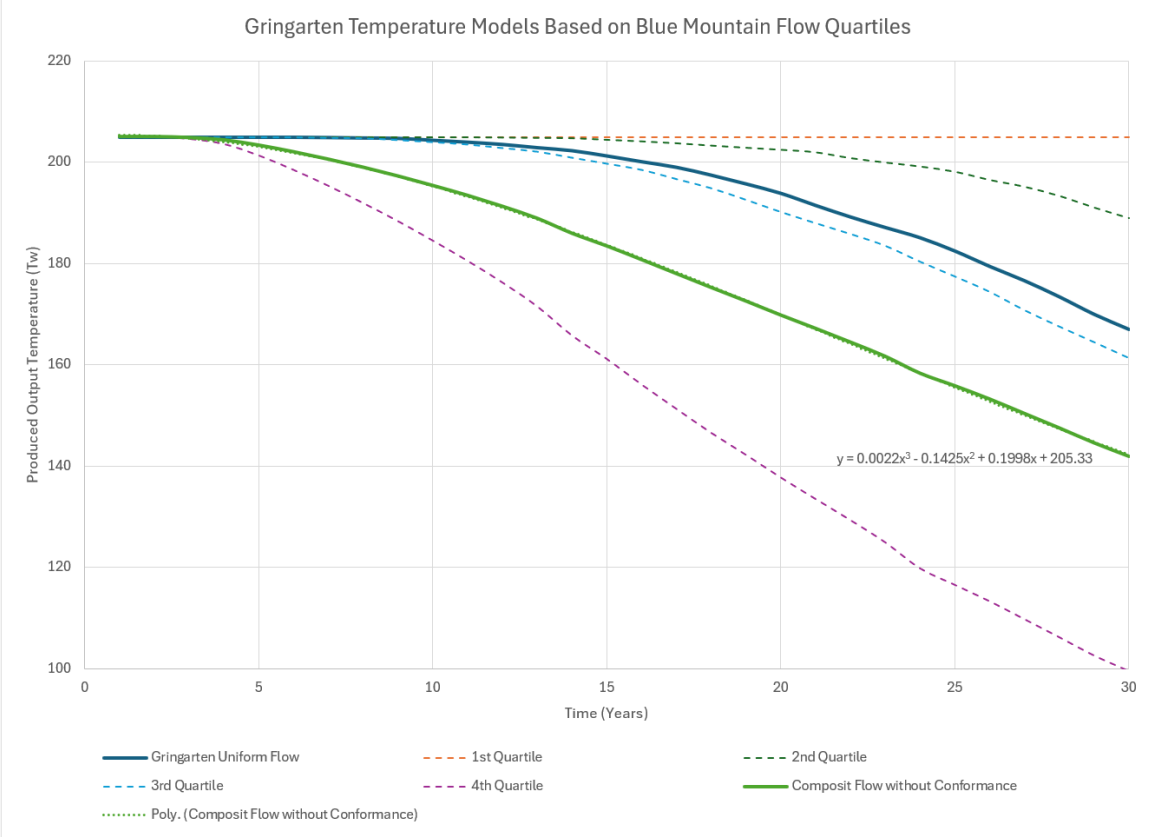

Figure 14: Gringarten temperature models based on Blue Mountain flow quartiles.

Using Figure 14, the impact of the short circuiting can be visualized with three areas that are of major concern. First, the composite decline curve for short-circuiting starts considerably earlier, in this case as early as year 3 with short-circuiting vs. year 10 with conformance control. Second, the rapid separation of the short-circuiting composite curve causes the short circuit system to reach the 25˚C decline mark 10 years earlier than conformance control curve. Third, the 1st and 2nd quartiles (50%) of the resource show limited heat harvesting in the first 20 years and essential no heat harvesting for the duration of the project in the 1st quartile.

The impact on power production follows the same trends. Figure 15 examines the Gringarten models for the system given conformance as well as short circuits. The calculations use a plant up time of 90%, the power conversion factors discussed earlier of 4.36E-07 MW-hr / (˚C·BWPD), 8% ORC plant parasitic loads, and the temperature predictions from Figure 14. The short circuit's temperature drops below the critical 3.0 MW of electricity generating capability by year 15 and generates 26% less total electricity during the 30-year life of the plant.

2.8. Introduction to "Perf and Plug" vs. Sleeves

Similar to Blue Mountain, the standard completion design for EGS has defaulted to the "Perf and Plug" technique. This has been used exclusively at Project Cape as well as all non-open hole stimulation at Forge. There are significant advantages to "Perf and Plug" that has made it a favorite among completion engineers, the largest being cost. Thanks to the advancements in the shale boom from the early 2000's through today, the cost have dropped significantly for this technique. Additionally, the reliability of the perforating guns and the plugs has improved.

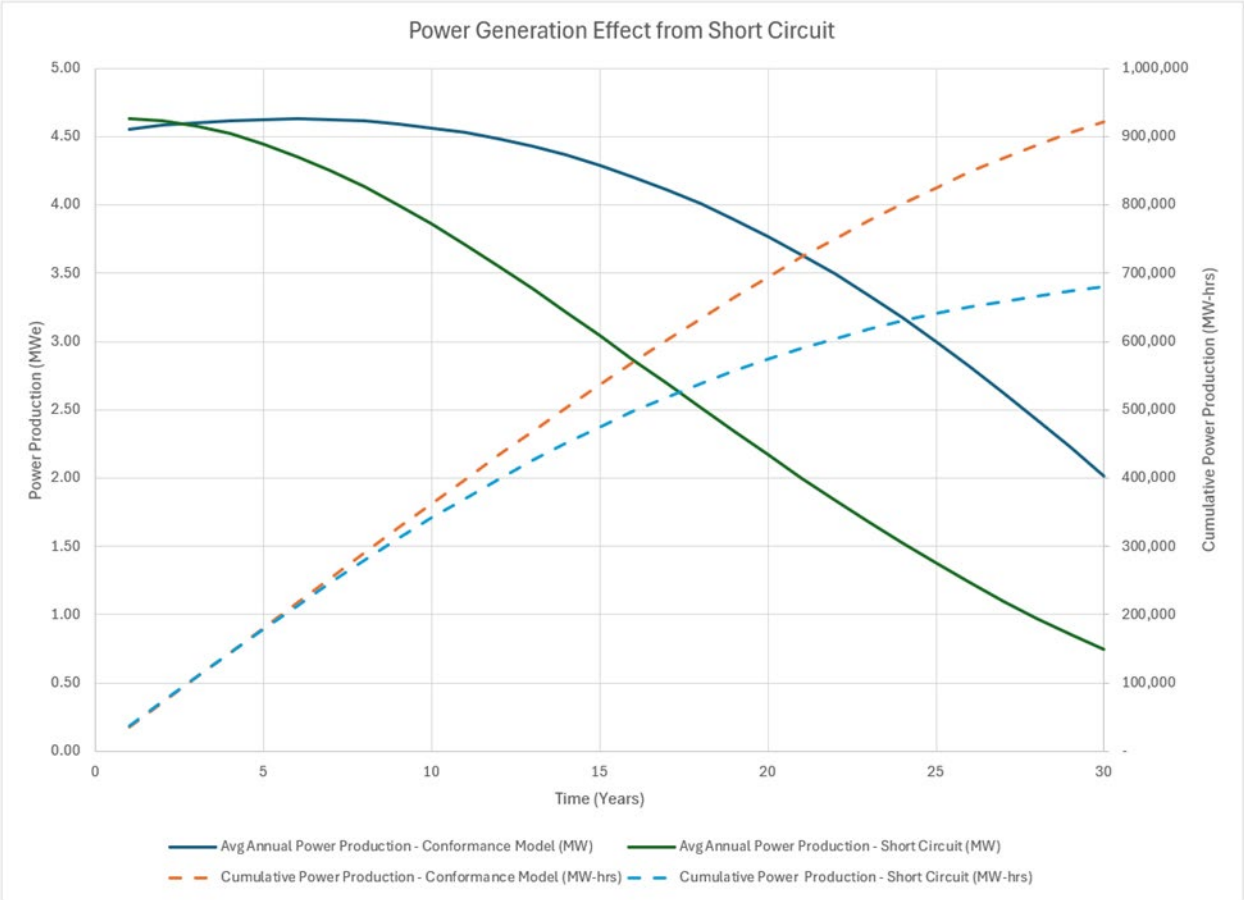

Figure 15: Power generation differences between conformance control and short circuits.

Unfortunately, "Perf and Plug" comes with a major disadvantage. Once perforations are shot through the casing and fracture stimulated, the only effective way to shut them off or slow down injection through the short circuits is to run an inner-string with multiple packers and outflow control devices (OCD). A typical conformance design using inner-string consists of the original 7" casing, perforated and stimulated in 50-150 locations down the wellbore. A 4" inner-string would be run across the injection interval using a packer to separate each stage with an OCD located between each packer to control flow into each interval where there is a short circuit.

Unfortunately, this system has two major drawbacks. First are the frictional losses described in the Nodal Analysis section increase over 17 times at injection temperatures and 1,500 gpm. Second the reliability of packers is unproven at these temperatures, compounded by the cyclic loading of cool (150˚F) injection temperature followed by 400˚F reservoir temperatures during shut in periods.

The oil and gas industry has tried to use gels, cement, and other chemicals to manage injection conformance control over the years, all with very limited success. The combination of difficulty using this technology to manage conformance in 3,000-8,000 BPD injectors at 150˚F, with the increase in difficulty of EGS requiring 60,000-120,000 BPD at temperatures in excess of 400˚F creates significant doubt in the viability of these options in EGS.

The alternative to "Perf and Plug" that is currently used in the shale market, predominately in Canada, is the frac sleeve technology. The advantage to the frac sleeve is that if the sleeve is designed properly, the sleeve and be shifted back into the closed position to shut off a short circuit without giving up internal diameter in the casing and inadvertently increasing friction pressure and parasitic losses.

Additionally, technology is being investigated that will allow for an OCD to be built directly into the sleeve allowing for a regulator position that will limit the injection into short circuits, preventing the premature cooling of the system, but still allowing for the heat to be harvested from that section of the reservoir.

2.9. Modeling the Impact of Inner-Strings on Friction

Using the same flow loop as described in the Nodal Analysis section the only realistic ability to implement conformance control in Perf and Plug is with an Inner String. Figure 16 is a graphical depiction of how a 4" Inner-String system would look in 7" casing.

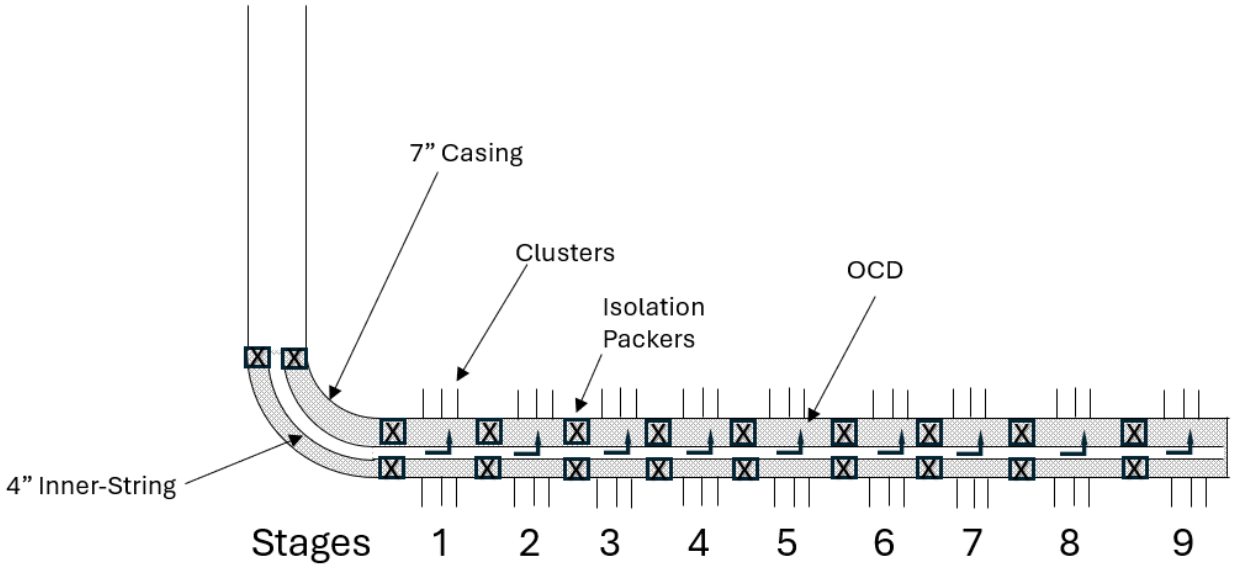

Figure 16: 4" Inner-string in 7" casing with outflow control devices.

Returning to the Nodal Analysis described earlier for the hypothetical doublet using 7" casing in both the producer and injector, 55 frac stages and 56,000 BWPD, the system required 3,130 HP. Assuming the same system, but on the injector only, there is a 4" conformance inner string run from the top of the 1st stage (10,930 ft MD) to the bottom of the well (17,765 ft MD) the power requirement to circulate the water jumps to 6,207 HP. Converting this to power with an 80% pump efficiency results in 5.8 MW, or 115% of the power produced.

$$MW_e = \frac{HHP \times 0.000745699}{\eta_{pump}} \tag{10}$$

This exercise shows quickly that if "Perf and Plug" is chosen as the completion alternative, then there is not an economic alternative for conformance control.

Alternatively, the ability to maintain full bore with the sleeves and having the ability to shut off short circuits or in the future be able to install regulator positions within the sleeves will allow for a system of conformance control without significant impact on the economics.

2.10. Parasitic Loads for Different Well Architecture

Using the same flow loop as described in the Nodal Analysis and the Impact of Inner-Strings on Friction an analysis was performed of different wellbore architectures. The reason for performing a deep dive on these variables is the theoretical EGS system that was analyzed in this paper assumed the Blue Mountain design with 7" long strings of casing in both the injector and the producer. This design indicated that to circulate 56,000 BWPD for 55 stage EGS with 144' spacing, the system would require 3,130 HP. This is the equivalent of 2.9 MW of electricity or 58.3% of the electricity generated prior to plant parasitic losses. Table 4 examines the parasitic losses as a function of the wellbore architecture. The critical insight gained from this data is that for the required rates to generate greater than 5 MWe per well, the friction of the system becomes a dominant variable. The numbers for production and injection 7" long strings are consistent with Blue Mountain in Norbeck (Norbeck and Latimer 2023), where parasitic losses of 0.5 to 1.0MW were observed in a considerably shorter (~2,400') injection interval and using lower rates (800 GPM or 27,000 BWPD Injected). The model used for this paper estimated 0.6 MW of parasitic losses for Blue Mountain at 800 gpm.

Table 4: Parasitic Losses as a Function of Well Design

Injector Architecture	Producer Architecture	Doublet / Triplet	Injection Rate (BWPD)	Friction Losses (psi)	Parasitic Losses (MWe)
7" Long String	7" Long String	Doublet (5MWe)	60,480 (8% fluid loss)	3,041 psi	2.9 MWe
7" Long String + 4" Inner-string	7" Long String	Doublet (5MWe)	60,480 (8% fluid loss)	6,031 psi	**5.8 MW**
9-5/8" x 7" Liner	9-5/8" x 7" Liner	Doublet (5MWe)	60,480 (8% fluid loss)	1,426 psi	1.4 MW
9-5/8" x 7" Liner + 4" Inner-string	9-5/8" x 7" Liner	Doublet (5MWe)	60,480 (8% fluid loss)	4,416 psi	4.2 MW
9-5/8" x 7" Liner	9-5/8" x 7" Liner	Triplet (10MWe)	120,960 (8% fluid loss)	2,639 psi	5.1 MW
7" Long String	7" Long String	Triplet (10MWe)	120,960 (8% fluid loss)	6,847 psi	**13.1 MW**

Critical insight gained from this modeling effort is the impact of the 7" long string as compared to using a 9-5/8" casing set above the resource with a 7" liner through the resource interval. This change in design can reduce the parasitic loads by over 50%. Additionally, without converting to

a casing / liner design or increasing bore sizes considerably to an 8-5/8” or 9-5/8” long string, the frictional impact for the triplet’s flow rate is detrimental to the economics of the project.

There are multiple reasons why casing long strings can be preferred, including operational efficiency and the ability to run fiber optics. However, all advantages of a long string over a liner must be weighed against the cost of the parasitic losses incurred with the additional friction vs. a liner.

3. Conclusions

1. Generation of geothermal electricity in the United States has stagnated between 1.5 GW and 1.9 GW since 1990. The primary cause of this stagnation is the lack of new hydrothermal reservoirs discoveries.
2. To grow geothermal power generation, geothermal power generation using Enhanced (or Engineered) Geothermal Systems (EGS) has tremendous potential. New technologies are being developed to provide economies of scale and low thermal declines needed to provide economic power generation.
3. Key variables impacting the economics of EGS power generation are the thermal decline, flowrate per well, parasitic losses and success of conformance control.
4. Parasitic losses are defined as the electricity used to power a geothermal field and power plant that does not contribute to the net electric power yield of a plant for transmission.
5. Frictional losses in the wellbore and in hydraulic fractures across various well completions geometries must be optimize for an economic EGS development.

Appendix

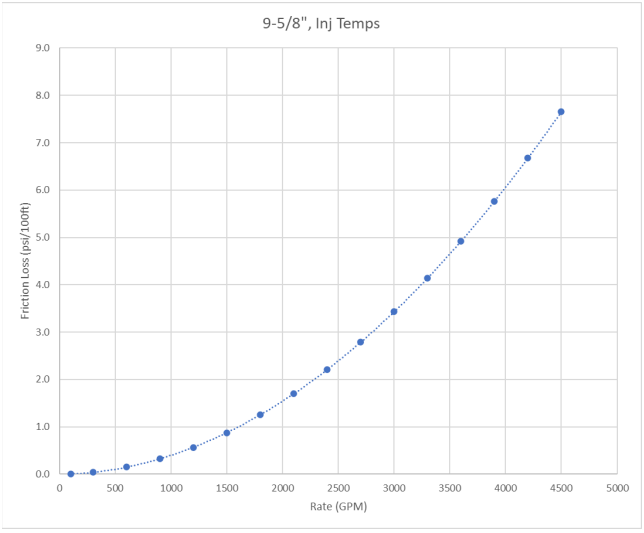
9-5/8", Inj Temps
Friction Loss (psi/100ft)
Rate (GPM)
0.0
1.0
2.0
3.0
4.0
5.0
6.0
7.0
8.0
9.0
0
500
1000
1500
2000
2500
3000
3500
4000
4500
5000

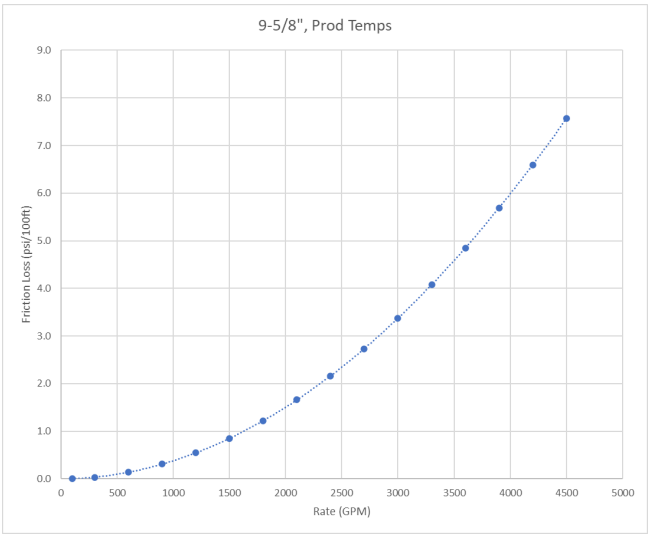
9-5/8", Prod Temps
Friction Loss (psi/100ft)
Rate (GPM)
0.0
1.0
2.0
3.0
4.0
5.0
6.0
7.0
8.0
9.0
0
500
1000
1500
2000
2500
3000
3500
4000
4500
5000

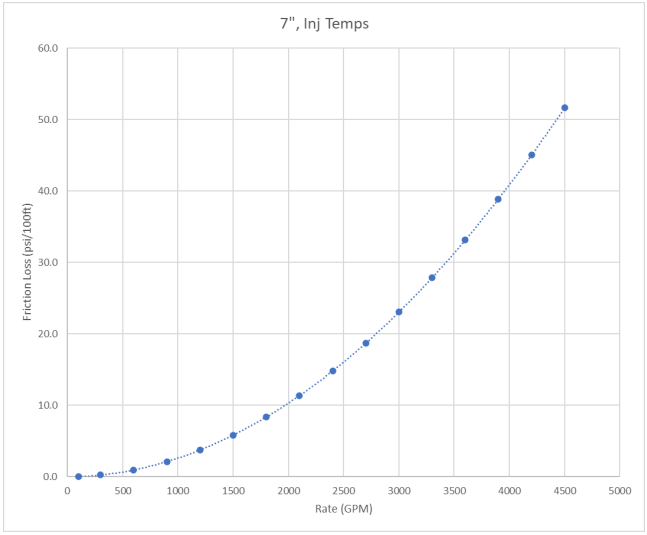
7", Inj Temps
Friction Loss (psi/100ft)
Rate (GPM)
0.0
10.0
20.0
30.0
40.0
50.0
60.0
0
500
1000
1500
2000
2500
3000
3500
4000
4500
5000

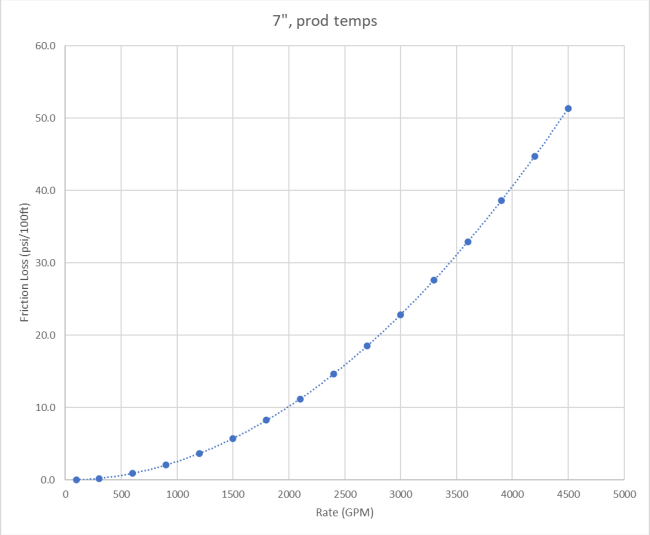
7", prod temps
Friction Loss (psi/100ft)
60.0
50.0
40.0
30.0
20.0
10.0
0.0
0
500
1000
1500
2000
2500
3000
3500
4000
4500
5000
Rate (GPM)

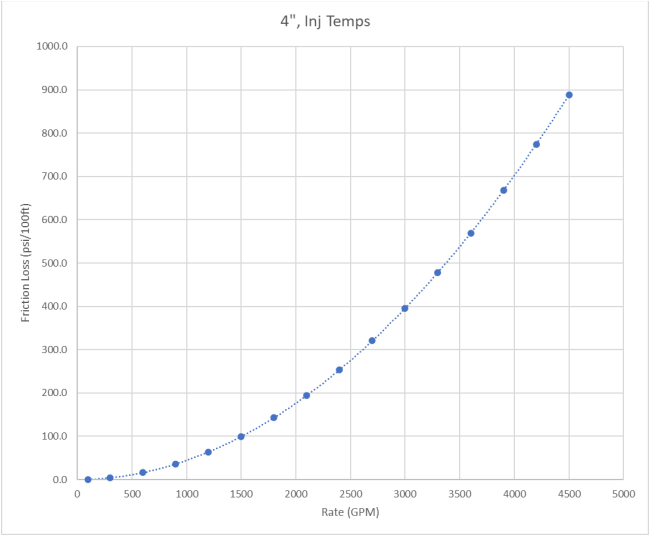
4", Inj Temps
Friction Loss (psi/100ft)
1000.0
900.0
800.0
700.0
600.0
500.0
400.0
300.0
200.0
100.0
0.0
0
500
1000
1500
2000
2500
3000
3500
4000
4500
5000
Rate (GPM)

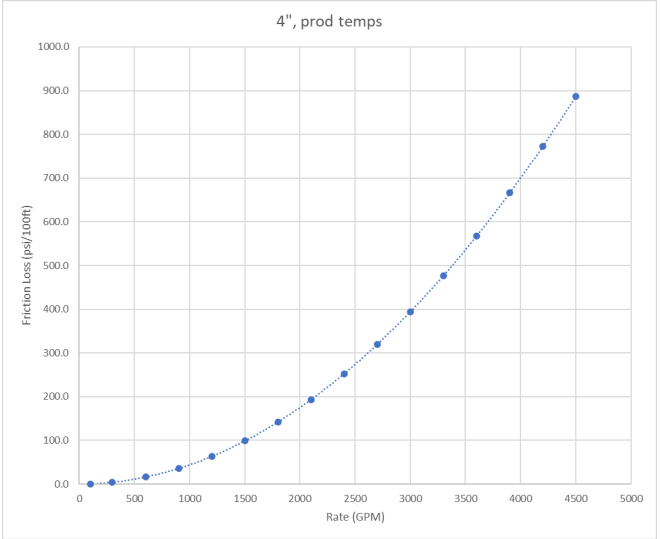
4", prod temps
Friction Loss (psi/100ft)
1000.0
900.0
800.0
700.0
600.0
500.0
400.0
300.0
200.0
100.0
0.0
0
500
1000
1500
2000
2500
3000
3500
4000
4500
5000
Rate (GPM)

Acknowledgement

This material is based upon work supported by the Department of Energy, Office of Energy Efficiency and Renewable Energy (EERE), under Award Number DE-EE0007080. This report was prepared as an account of work sponsored by an agency of the United States Government. Neither the United States Government nor any agency thereof, nor any of their employees, makes any warranty, express or implied, or assumes any legal liability or responsibility for the accuracy, completeness, or usefulness of any information, apparatus, product, or process disclosed, or represents that its use would not infringe privately owned rights. Reference herein to any specific commercial product, process, or service by trade name, trademark, manufacturer, or otherwise does not necessarily constitute or imply its endorsement, recommendation, or favoring by the United States Government or any agency thereof. The views and opinions of authors expressed herein do not necessarily state or reflect those of the United States Government or any agency thereof.

REFERENCES

Augustine, Chad. 2016. "A Methodology for Calculating EGS Electricity Generation Potential." Golden, CO: GRC Transactions, Vol. 40, 2016.

Augustine, Chad. 2011. Updated U.S. Geothermal Supply Characterization and Representation for Market Penetration Model Input. Golden, CO: National Renewable Energy Laboratory.

Banks, Jonathan, Arif Rabbani, Kabir Nadkarni, and Evan Renaud. 2020. "Estimating parasitic loads related to brine production from a hots Sedimentary aquifer geothermal project: A case study from the Clarke Lake gas field, British Columbia." (Renewable Energy, ELSEVIER) (153).

DiPippo, Ronald. 2016. Geothermal Power Plants, 4th edition. Waltham, Ma: Butterworth-Heinemann / Elsevier.

Doe, Thomas, Robert McLaren, and William Dershowitz. 2014. "Discrete Fracture Network Simulations of Enhanced Geothermal Systems." Stanford, CA: Thirty-Ninth Workshop on Geothermal Reservoir Engineering.

Fleckenstein, William, Kazemi Hossein, Royer Colby, Loff Geneva, and Zimmermann Jens. 2023. "A Stochastic Economic Analysis of An Enhanced Geothermal System." Golden Colorado: GRC Transactions, Vol. 47, 2023.

Geiser, Pater, Bruce Marsh, and Markus Hilpert. 2016. "Geothermal: The Marginalization of Earth's Largest and Greenest Energy Source." Stanford, California: 41st Workshop on Geothermal Reservoir Engineering.

Gringarten, W. A., A. P. Witherspoon, and Y. Ohnishi. 1975. "Theory of Heat Extraction from Hot Dry Rock." (Journal of Geophysical Research) 80, 1120-1124.

Mindygaliyeva, Balnur, Ozan Uzun, Kaveh Amini, Kazemi Hossein, and William Fleckenstein. 2024. "Assessment of Two Recent Hot Dry Rock Thermal Energy Production Projects." (Geothermics).

MIT led interdisciplinary panel. 2006. The Future of Geothermal Energy; Impact of Enhanced Geothermal Systems (EGS) on the United States in the 21st Century. Idaho Falls, ID: Idaho National Laboratory.

Moon, Hyungsul, and Sadiq J. Zarrouk. 2012. "EFFICIENCY OF GEOTHERMAL POWER PLANTS: A WORLDWIDE REVIEW." Auckland, New Zealand: New Zealand Geothermal Workshop 2012 Proceedings.

Norbeck, Jack H., and Timothy M. Latimer. 2023. "Commercial-Scale Demonstration of a First-of-a-Kind." Houston, TX: EarthArXiv.

Pearson, C. Mark. 2001. "Dimensionless Fracture Conductivity, Better Input Values Make Better Wells." (Journal of Petroleum Technology) (January, 2001).

Robins, Jody C., Amanda Kolker, Francisco Flores-Espino, William Pettitt, Brian Schmidt, Koenraad Beckers, Hannah Pauling, and Ben Anderson. 2021. 2012 U.S. Geothermal Power Production and District Heating Market Report. Golden, CO: National Renewable Energy Laboratory.

Titov, Aleksei, Jack Norbeck, Sireesh Dadi, Katharine Voller, Mark Woitt, Steven Fercho, Emma McConville, et al. 2023. "Case Study: Completion and Well Placement Optimization Using Distributed Fiber Optic Sensing in Next-Generation Geothermal Projects." (Unconventional Resource Technology Conference).